LBL-28264
UC-411

Lawrence Berkeley Laboratory
UNIVERSITY OF CALIFORNIA

Accelerator & Fusion Research Division

Heavy Ion Fusion Accelerator Research (HIFAR)
Year-End Report, April 1, 1989 – September 30, 1989

Heavy Ion Fusion Staff

December 1989

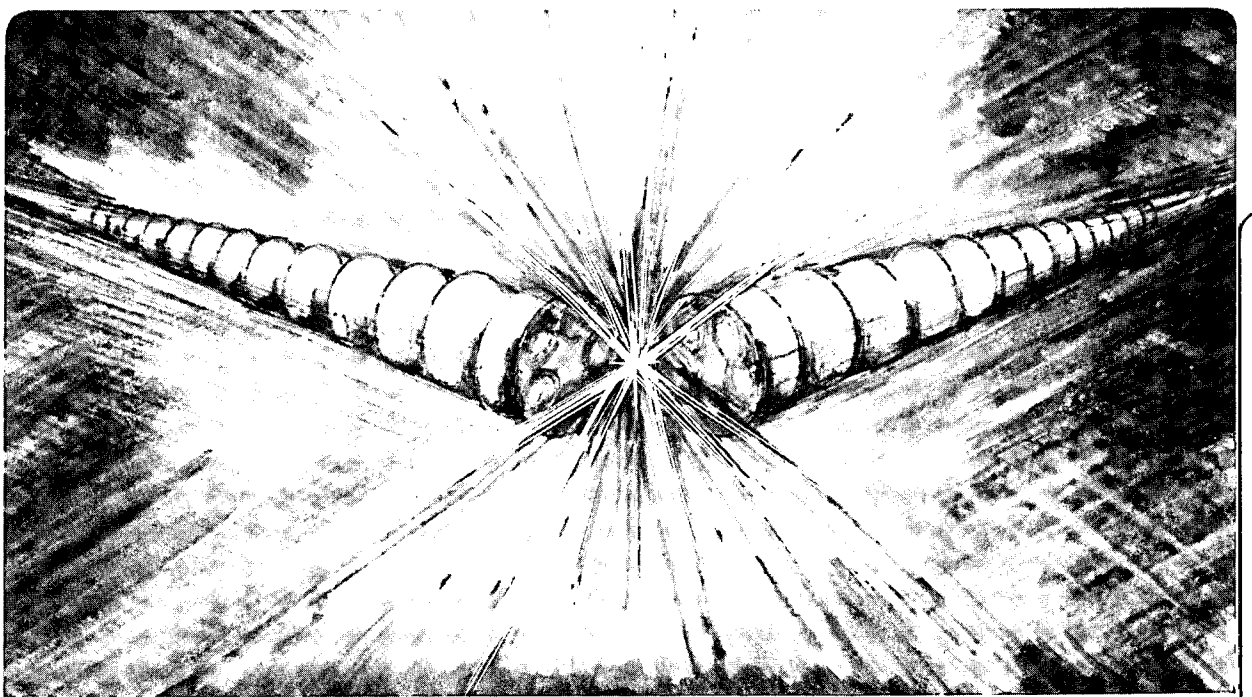

Prepared for the U.S. Department of Energy under Contract Number DE-AC03-76SF00098.

DISCLAIMER

LBL-28264
HIFAN-442

HEAVY ION FUSION ACCELERATOR RESEARCH (HIFAR)

YEAR-END REPORT*

April 1, 1989 - Sept. 30, 1989

Heavy Ion Fusion Staff

Accelerator and Fusion Research

Lawrence Berkeley Laboratory
1 Cyclotron Road
Berkeley, CA 94720

December 1989

* This work was supported by the Director, Office of Energy Research, Office of Basic Energy Sciences, Advanced Energy Projects Division, U.S. Department of Energy under Contract No. DE-AC03-76SF00098.

FOREWORD

The basic objective of the Heavy Ion Fusion Accelerator Research (HIFAR) program is to assess the suitability of heavy ion accelerators as igniters for Inertial Confinement Fusion (ICF). A specific accelerator technology, the induction linac, has been studied at the Lawrence Berkeley Laboratory and has reached the point at which its viability for ICF applications can be assessed over the next few years.

The HIFAR program addresses the generation of high-power, high-brightness beams of heavy ions, the understanding of the scaling laws in this novel physics regime, and the validation of new accelerator strategies, to cut costs. Key elements to be addressed include: 1) Beam quality limits set by transverse and longitudinal beam physics; 2) Development of induction accelerating modules, and multiple-beam hardware, at affordable costs; 3) Acceleration of multiple beams with current amplification -- both new features in a linac -- without significant dilution of the optical quality of the beams; 4) Final bunching, transport, and accurate focussing on a small target.

TABLE OF CONTENTS

HIGHLIGHTS

D. Keefe

1. Mid-way through this reporting period, the National Academy of Sciences' ICF Review Panel began their series of meetings. Significant effort has gone into preparation of presentational material and briefing documents relevant to their deliberations. The Panel's preliminary report is due in January, 1990, and their final report in September, 1990. Their judgment on the role of HIFAR, the only one of the inertial fusion programs exclusively devoted to the energy application, could have a significant effect on the future course of the HIFAR program.

2. Understanding of the transverse beam dynamics in the MBE-4 experiment is still not complete, and this issue has taken considerably more effort and time than anticipated. While there is no evidence for growth in normalized emittance in the 10-mA drifting (i.e., unaccelerated) beam passing through the length of the accelerator, this is not the case for the beam when it undergoes acceleration accompanied by current amplification. In the latter case, some growth (< 50%) is predicted by our numerical simulations of the apparatus because the electrostatic beam energy changes as the beam is compressed; the scaling of this effect is known, and is not significant for driver parameters. The total overall growth experimentally from front to end (roughly a factor of two), however, seems to be more than this ; so far, understanding of the discrepancy has eluded both our experimental and theoretical efforts.

   While the discrepancy is small, we believe it to be real as measured in terms of root-mean-square emittance. The experimental studies are, indeed, challenging: the accelerator is rather short with only a small change in ion velocity (<2); the emittance is very small and space-charge effects large, thus demanding quite unusual precision in measurement. Each experimental run is accompanied by extensive calibration procedures, e.g., checking the

single-particle betatron tune or establishing that the beam is correctly matched at all observation points.

In an effort to shed light on the issue, the post-extraction geometry has been modified to select the more uniform core of the 10-mA beam. The current is thereby decreased to 5 mA with a drop in emittance also by a factor of two, resulting in a beam of higher brightness (i.e., even more dominated by space-charge effects, with $\sigma/\sigma_0 = 6°/72° = 0.083$). Preliminary results on the drifting 5-mA beam are reported.

In parallel, an improved geometry for the injection diode is being designed which when implemented should result in a more uniform 10-mA beam from the 200-kV injector.

3. Following an earlier successful "preview" check on the 2-MV Injector (with only 10 of the 18 Marx trays installed) to established that the dome would not break down to the wall at 2 MV, the installation of the final 8 trays has been completed. In addition, machining of the 16-beam electrodes is complete. Voltage-holding tests of the ceramic 16-beam column are under way.

Power for the sources and associated electronics will be provided by a 3.5-kW alternator mounted in the high-voltage dome. The original concept of driving the alternator by a rotating lucite shaft running the length of the Marx generator has been abandoned in favor of a hydraulic drive; preliminary tests on this system have been very encouraging.

Borrowing from the control philosophy for the Advanced Light Source at present under construction, we have begun instituting the Injector Control System. An intelligent local controller (ILC) is now operating to monitor voltages with the data displayed on an IBM AT computer.

4. The carbon - source program has now been mainly concentrated on improving the lifetime and reliability of the sources. Three directions being systematically explored are a) small modifications to the design geometry, b) substitution of different materials (e.g., in the trigger electrode), and c) non-invasive methods of refurbishing a faulty source (e.g., by glow-discharge cleaning in place). Early tests show mean-time to failure of ~ 10^4 shots, where "failure" is defined as a drop in reliability from > 99% to about 90%.

5. In another off-line program to improve the purchased trigger-gaps for the 2-MV generator, the lifetime has been increased from about 10^5 shots to some 10^6 shots.

6. The ILSE engineering study pointed up the need for component R and D for elements needed in future HIFAR experiments. This activity, which has proceeded at relatively low level, has resulted in fabrication of a 16-beam electrostatic-quadrupole array to establish how well the assembly method can meet the tight imposed tolerances and, also, to determine its high-voltage-breakdown characteristics. Additional effort has been devoted to design efforts on current-dominated magnetic lenses of the Cos-2θ type and to design and sub-assembly tests of an accelerator cell.

7. Stabilization of the longitudinal instability in a driver can be achieved by introducing momentum spread which, in turn, can lead to a more complicated final-focus system to avoid chromatic effects. Other stabilizing mechanisms can exist, such as arranging for the parallel accelerated beams to have unequal currents. This is found to help increase the growth length, perhaps at the price of rather significant imbalance among the beam currents.

8. Development of a new cost-optimization code (HILDA) is continuing at a low level.

MBE-4 DRIFTING BEAM QUADRUPOLE OPERATING RANGE

H. Meuth and S. Eylon.

The MBE-4 quadrupole voltage operating range was measured, so that the window of operation with respect to mismatch and phase advance could be determined. The measurements were done on a single 10 mA drifting beam to eliminate any beam-beam interaction (the other three beams were disabled at the source). The beam parameters; current, rms un-normalized transverse emittance, divergence angle, radius, and centroid position and angle, were taken at LP15 (middle of the MBE-4 accelerator) using the double-slit emittance scanner and Faraday cups to measure current.

As shown in Fig. 1 the normalized transverse emittance in the vertical direction (minor axis "x") is not sensitive to variations in quadrupole voltage V_q within the range of 16 kV to 22 kV. This corresponds to a variation in σ_o phase advance[1] from 60^o to 90^o. The emittance is not sensitive to a wide range of mismatch in the beam (a factor that was previously thought[2] to contribute to the transverse emittance growth observed in the accelerated beam). The emittance in the horizontal direction (major axis "y") (as shown in Fig. 3 was also found to be insensitive to beam mismatch and was about equal to the emittance measured in the vertical direction (x). For these measurements, the vertical beam coherent betatron oscillations shown in Fig. 2 had an offset amplitude $\langle x \rangle_{max}$ of 1 mm in position and $\langle x' \rangle_{max}$ of 6 m-rad in angle. These amplitudes correspond to a change of $\delta V_q = 3$ kV in the quadrupole voltage in agreement with a change in the total phase advance of 180^o between LP0 and LP15.

The total beam current at B-15 as measured with a Faraday cup as a function of V_q is given in Fig. 4. One observes a constant current for 16 kV< V_q< 21 kV corresponding to the range where the emittance was found to be "flat". Outside that range the current drops and the emittance grows.

References:

1. H. Meuth, S. Eylon, E. Henestroza and K. Hahn, "Zero-current phase advance measurements in MBE-4." Half year report: LBL-27230, UC-411.

2. H. Meuth and K.D. Hahn, S. Eylon and L. Smith, "A detailed study of transverse emittance in MBE-4." Half year report: LBL-27230, UC-411.

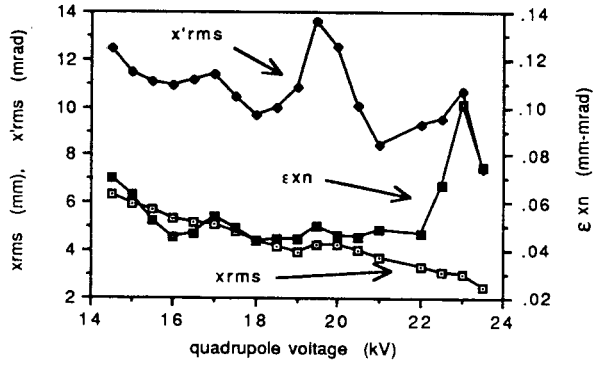

Fig. 1 Top beam vertical ms radius x, angle x' and normalized emittance εxn (@ 80% level) at LP15 vs. quadrupole voltage.

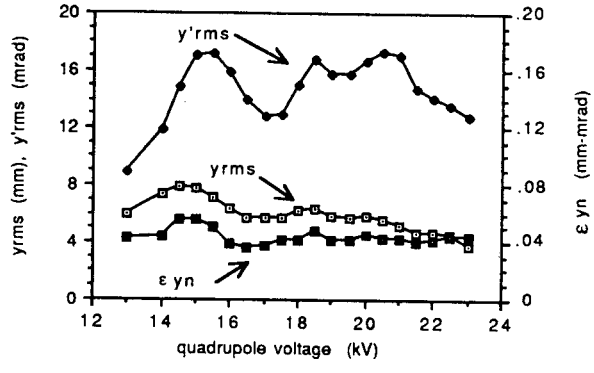

Fig. 3 Top beam horizontal ms radius y, angle y and normalized emittance εyn (@ 80% level) at LP15 vs. Vq.

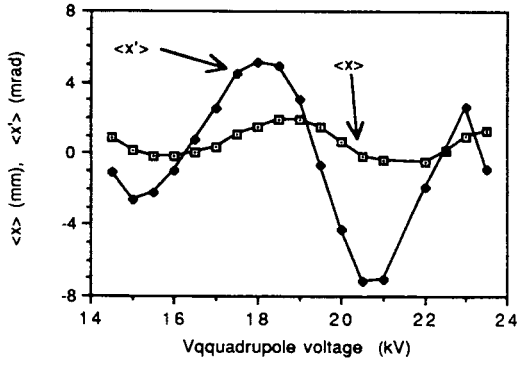

Fig. 2 Top beam vertical transverse oscillations of position <x> and angle <x'> centroid (@ 80% level) at LP15 vs Vq.

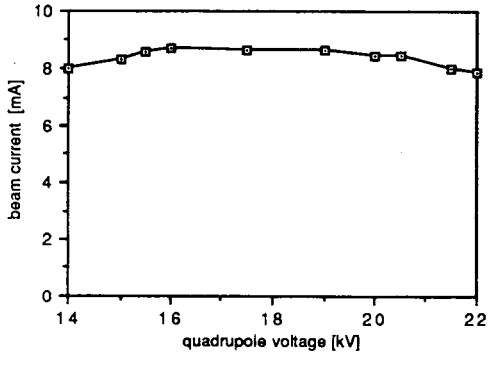

Fig. 4 Top beam current (@ center of the pulse at LP15 vs quadrupole voltage.

TRANSVERSE EMITTANCE GROWTH IN MBE-4

T.J. Fessenden and K.D. Hahn

For the past year or more the MBE-4 experiments have indicated that the acceleration process causes the normalized emittance of the MBE-4 beams to increase. These emittance measurements are very difficult to perform and as a consequence the experimental error in the data is relatively large. Very careful experiments, reported[1] in the last semi-annual HIFAR report, focused on emittance growth with acceleration in the first half of MBE-4. Simulations[2] of these experiments using an upgraded version of Haber's SHIFTXY code also showed emittance growth but by amounts insufficient to explain the experimental data. More recently, simulations using smaller initial emittances that approached the "intrinsic" emittance of the beam (see Eq. 1) showed much better agreement with the experiments.

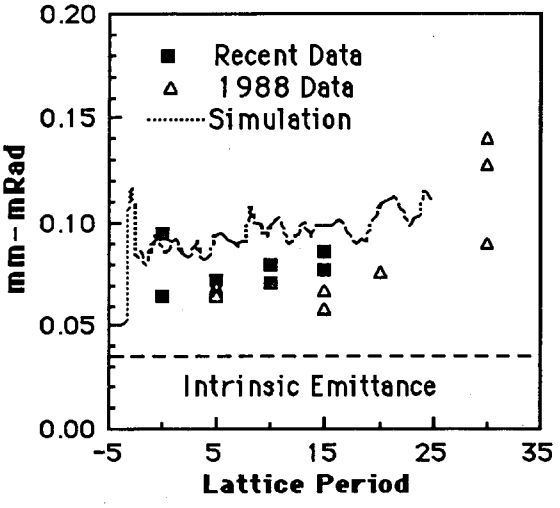

Fig. 1 Comparison of measurements of the norm-alized emittance of accelerated MBE-4 beams with the SHIFTXYA simulation

Figure 1 is a plot of the MBE-4 emittance measurements compared with a very recent simulation using the SHIFTXYA code. In the notation of MBE-4, the matching section extends from LP-4 to LP 0 and the accelerator extends from LP 0 to LP30. The initial currents for these measurements is the nominal 10 mA used in most of the MBE-4 experiments. The "Recent Data" was reported in reference 1. The "1988 data" was taken in the summer and fall of 1988. Also shown is the "intrinsic" emittance of the beams given by

$$\varepsilon_i = 2b\frac{v_\theta}{c} \qquad (1)$$

Here b is the radius of the source (2 cm), v_θ is the ion thermal velocity due to the temperature of the source (corresponds to 0.1 eV) and c is the velocity of light. The simulation assumed an initial normalized emittance of 0.05 mm-mRad. An important difference is that the simulation used 100% of the particles to calculate emittance whereas the experiment used only 90% to reduce the effects of noise. The simulation results are shown by the dotted curve in Fig. 1.

An analytic theory[3] of emittance growth under acceleration was developed by Hahn and Smith. This work, which extends the usual emittance formula[4] to include effects due to acceleration and compression, is in good agreement with the simulation, e.g., both predict the slow rise by ~15% as the beam length compresses. If the MBE-4 experiments could further confirm this theory, it could be used with increased confidence to understand transverse emittance growth in a fusion driver.

Earlier emittance measurements, reported[5] at the 1987 PAC meeting, showed no normalized emittance growth with acceleration. These measurements used instruments considerably inferior to those presently in use and produced emittance values greater than 0.2 mm-mRad . At these large emittance values a computer simulation would undoubtedly predict a much smaller relative emittance growth which could easily have been missed. There is evidence that the beam emittance had been degraded in the matching section to values near 0.2 mm-mRad in these early experiments.

The experiments on MBE-4 are now directed toward validating the analytic theory over longer acceleration lengths. Experiments are proceeding with an initial current of 4.5 mA per beam using the improved ion source described in the next paper.

References

1. H. Meuth, K.D. Hahn, S. Eylon, and L. Smith. HIFAR Half-Year Report LBL-27230, p. 6, Oct.-Mar. 1989.
2. K.D. Hahn and L. Smith, HIFAR Half-Year Report LBL-26482, p.9, Apr.-Sep. 1988.
3. K.D. Hahn and L. Smith, "2-D Emittance Equation with Acceleration and Compression" LBL-26167, Oct. 1988
4. See for instance T.P. Wangler, K.R. Crandall, T.S. Mills, and M. Reiser, IEEE Trans. Nucl. Sci. **NS-32**, 2196 (1985).
5. T.J. Fessenden, D. Keefe, C. Kim, H. Meuth, and A. Warwick, IEEE Cat. No. 87CH2387-9, p. 898, (1987) also LBL-22217.

AN IMPROVED ION SOURCE FOR MBE-4

S. Eylon, E. Henestroza, H. Meuth

Recent studies of the transverse beam dynamics in the MBE-4 experiment suggested a possible contribution by the ion source characteristics to the normalized transverse emittance growth as observed in the accelerated beam measurements. [Ref.1]

The beam-dynamics characteristics, i.e., phase space and current density distributions, were determined experimentally using a pinhole/slitcup combination. The pinhole was placed at LP-4 between the steerer's exit and the first quadrupole entrance (as close as possible to the ion source exit). At this position the beam is still cylindrically symmetric. The slit cup is placed at LP-3 diagnostic station, after the first quadrupole set.

The phase space distribution of the 10-mA beam at LP-4 was shown in Ref.1. There one saw that the beam outermost rays were turned inward due to an overfocusing effect caused by field aberrations in the source diode. As a result current accumulated at the beam edge causing the beam current density profile to be hollow [Ref.1]. Those observations were in agreement with recent EGUN calculations.

A simple way for eliminating the outermost beam rays is by using a circular aperture ring (scraper) placed at the diode cathode plate, thus losing some of the beam current to the scraper. EGUN simulations were used to optimize the scraper diameter (beam quality vs. current). In a first approach we have installed the scraper at the cathode plate. Beam current waveforms measurements taken with a Faraday cup at LP-2 showed a deterioration in the waveform, namely a significant increase in the rise time and total current. It was suggested that this measured current increase is due to additional secondary electrons emitted from the scraper and accelerated toward the anode. To recapture those secondary electrons we biased the scraper with a positive 4.5-kV d.c. voltage. Current waveforms of the beam at various bias voltages are given in Fig.1 . The scraper is recessed 0.8" from the diode exit to eliminate electric field effects due to the bias voltage.

The beam characteristics, i.e., phase space and current density distributions at various scraper diameters (0.4", 0.45", and 0.5") were measured and found to be in agreement with EGUN calculations. An optimal scraper diameter of 0.45" was chosen leading to a current of 4.5 mA and a higher quality beam as shown in Fig. 2 and Fig. 3.

We are in the process of redesigning the diode to improve the optical quality of the 10 mA ion source. EGUN calculations indicate that 10 mA of beam with good emittance can be obtained by modifying the carbon plates and using a cupped ion source. Development of such a source has begun. We also plan to mechanically stabilize the diode geometry by connecting the carbon plates to the output aperture with four insulating posts.

References:

1. H. Meuth, K.D. Hahn, S. Eylon, and L. Smith. "A Detailed Study of Transverse Emittance in MBE-4". HIFAR Half-Year Report:LBL-27230,p.6, Oct.-Mar. 1989.

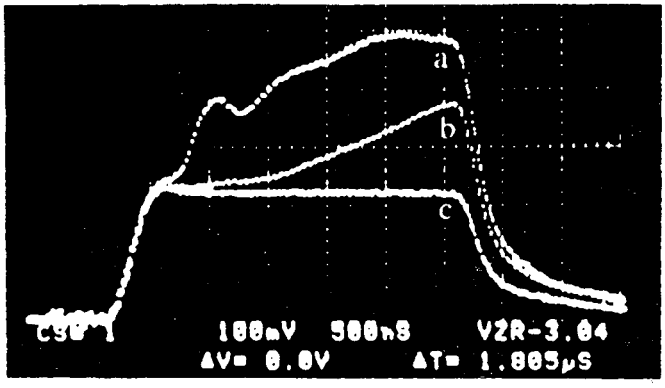

Fig. 1 Beam current into 50Ω with a scraper bias voltage of a) 0.75 kV, b) 2.75 kV, c) 4.75 kV.

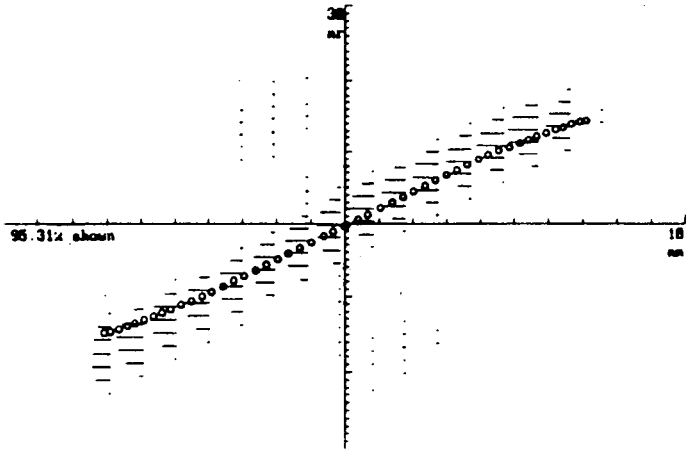

Fig. 2 Beam distribution in (x,x') space at point of injection into first quadrupole of matching section. Comparison between experiment (-) and EGUN code (o).

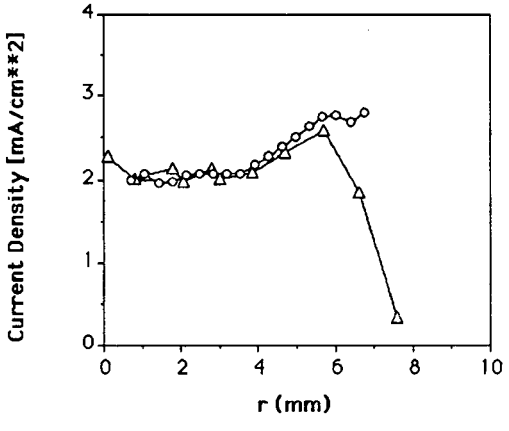

Fig. 3 Current density J(r) at point of injection into first quadrupole of matching section. Comparison between experiment (Δ) and EGUN code (o).

DRIFTING BEAM STUDIES ON MBE-4

T. Garvey and S. Eylon

Introduction

Previous studies[1] of the MBE-4 beam dynamics have been performed with a 10-mA beam which has a characteristic 'S' shaped emittance profile on emergence from the diode and which is accompanied by a rather hollow beam distribution. The phase space profile of this beam agreed well with that produced by simulations using the EGUN code and was understood in terms of diode aberrations acting on the outermost rays of the beam. In order to remove these rays from the transmitted beam, a biased aperture ring has been installed in one of the MBE-4 beam paths that allows only the relatively uniform central core of the ion beam to propagate into the beam matching. Results of studies of the biased aperture are discussed elsewhere in this report while here we discuss preliminary measurements of the transverse emittance of the reduced-aperture 4.5-mA beam.

Matching

The newly installed 0.45-inch diameter aperture resulted in a decrease in the nominal transmitted beam current from 10 mA to 4.5 mA. In order to compensate for the effect of reduced space-charge repulsion it was necessary to re-configure the matching section of MBE-4 by resetting the quadrupole voltages according to the values calculated using the in-house 'MATCH' codes. For the first attempt the quadrupole settings of the accelerating section were left at the values, used with the 10 mA beams which produce a 72 degree zero-current phase advance per period. The MATCH code was used to find envelope parameters at 4.5 mA for a matched beam in the 72° focusing channel. The matching section quadrupole voltage needed to match the measured parameters of the beam emerging from the diode to those needed at the input of the accelerating section were then calculated. Although there was good agreement between the measured and calculated values of size and divergence of the beam in the vertical plane at the exit of the matching section there was some discrepancy between the corresponding values for the horizontal plane. We are adding small physics effects to the MATCH codes and refining our experiments to improve the agreement between experiment and theory.

Results and Discussion

Figures 1 through to 3 show the variations of normalized r.m.s. emittance, beam size and divergence for the vertical plane (at the time of writing there are insufficient numbers of scanners to measure in both planes without breaking the machine vacuum). The values plotted pertain to 90% of the beam current. The effect of input mis-match is seen most clearly in Fig.3 where the divergence of the beam varies from one diagnostic station to the next. The beam size however stays fairly constant in the accelerating section (Fig.2) although the lower curve of figure 2 indicates that the beam centroid moves by almost two millimeters during its traversal of the linac. The emittance decreases initially from station 5 to stations 10 and 15 before steadily increasing towards the end of the machine. As we employ the r.m.s. definition of emittance the initial decrease is not forbidden in principle as the beam distribution may vary along the machine axis with higher order moments in the distribution flipping in and out. Indeed one can see some degree of filamentation in the phase space plots of the beam indicative of the particles sensing non-linear fields. The lowest value of emittance measured was 0.024 mm-mrad is lower than usually associated with the MBE-4 beam and is due to the reduced size of the 4.5 mA beams. The observed increase in emittance for the coasting beam is in contrast to previous observations[1] with the 10 mA beam in which the r.m.s. emittance stayed constant. However it is clear that the principal difference between these two sets of measurements lies in the extent to which the beam is matched. Future efforts will concentrate on improved matching to provide better conditions for studying the emittance behaviour of the drifting 4.5 mA beam before performing similar measurements on an accelerated 4.5 mA beam.

Reference

1. H. Meuth, K.D. Hahn, S. Eylon and L. Smith, "A Detailed Study of Transverse Emittance in MBE-4", HIFAR half year report (Oct. 88 - March 89), LBL-27230.

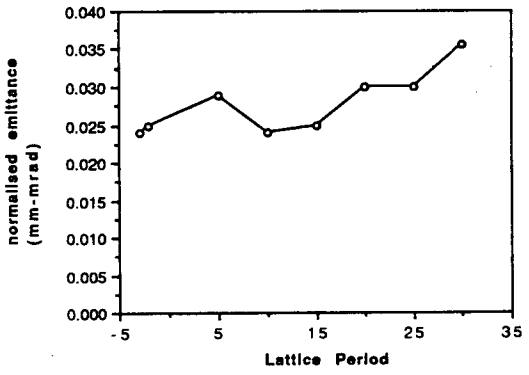

Fig. 1 Normalized emittance versus length in MBE-4.

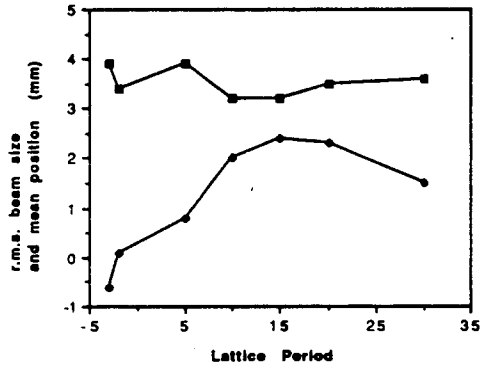

Fig. 2 Size and mean vertical position of a 5 mA beam through MBE-4.

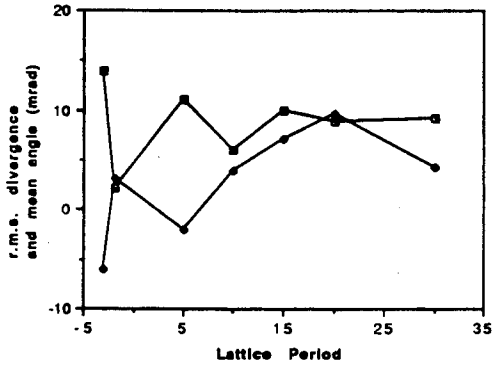

Fig. 3 RMS beam divergence and mean divergence angle through MBE-4.

2-MV INJECTOR

H. L. Rutkowski

H.V. Generator

In the last report period the ten-tray subsection of the inductively graded Marx was used to drive an open circuit. The system was rung up to 2 MV in an ambient atmosphere of 80 psig SF_6. This test established that the geometry of the system was satisfactory to operate at 2 MV with suitable gas pressure. This series of tests also established that terminal to ground breakdowns (these occurred under de-rated conditions) would result in serious damage to the generator mounting trays. The only practical way to protect the system from ground fault transients was to install two parallel strings of protection spark gaps down the system to provide a low inductance diversion circuit.

The full eighteen tray system was constructed with these protection gaps in place. Gaps were placed across each inductor as well as between inductors on opposite sides of the system. The gaps were set to a separation based on a controlled test at pressure in SF_6 so that they would arc over at 1.5 times the doubled capacitor charge voltage. Each inductor experiences the charge voltage on two capacitors instantaneously when the spark gaps fire. When the full eighteen tray system was fired at the 1-MV level into a dummy load, damage began to appear on the inductors which required extensive repair to the epoxy impregnated coils. There was no correlation between the damage and the age or location of a coil. After construction of the full eighteen-tray system the stable triggering window between self fire and the triggered firing limit became very narrow. The coils were repaired and the damage recurred. On many shots, the protection spark gaps fired randomly. The speculation that transients being developed by the protection gap discharges themselves might be destroying the coils led to removal of the protection gaps. After the coils were repaired again the system was tested to 1.3 MV without damage. The triggering of the system also improved somewhat.

We are designing more damage-resistant inductors and are investigating ways to reduce the effects of transients. We are also planning to modify the triggering circuitry.

Accelerating Column

The insulator modules were characterized for dimensional accuracy and cleaned in a new aluminum-oxide-bead blaster. The modules were characterized for circularity and flatness. The best module had a maximum deviation in circularity of .110" from an ideal axis. The flatness end to end was $\pm$ 1.1 mil. The equivalent numbers for the worst of the three modules were .159" concentricity and $\pm$ 3 mils flatness.

The cleaning process revealed contamination in the ceramic rings themselves. Before cleaning there was no visually apparent contamination. After cleaning, a circumferential, "tire tread" type pattern was observed which looked like it might be the result of some grinding process performed on the ceramic. Efforts to bead blast the pattern away were not successful although some 10 mils of ceramic were removed. Chemical analysis determined that magnesium, titanium, and iron were the main impurities. A representative from Coors Ceramics, the manufacturer determined that some of the ceramic rings had been smooth ground after grinding and that others had not. The modules were chemically treated at Los Alamos after brazing to remove surplus brazing material. Evidently some of the etched material was absorbed in the surface of the rings that were only rough ground. The dimensionally best module, which is being used for the up-coming 1-MV single-beam test was high-voltage tested in a bag of SF_6 at ambient pressure. The most contaminated section was D.C. tested with the appropriate H.V. hardware attached and with vacuum on the inside to 200 kV, which was the limit of the power supply. The maximum pulsed voltage on one section of a module is 175 kV in both the 1 and 2 MV versions of the system. Some clean sections were tested but breakdown on the outside of the module prevented us from getting above 140 kV D.C. These tests were terminated because we had no way of pressurizing the outside above 1 atm. The column will have to be conditioned in place in the injector pressure vessel.

The construction of the titanium electrodes which are presently being installed in the insulator module was a long process involving several outside companies. Essentially no problems occurred during the piece-part fabrication stage except for schedule slippage by the contractor. When the flat plate sections were laser welded to the conical sections, deflections of the flat plate occurred. Laser welding was deliberately chosen to avoid this problem. Several annealing treatments were used to bring the flatness within the $\pm$ .004" spec. Unfortunately, the hole locations were changed by this process and the two thin electrodes had to be re-machined. The thick electrodes were not a problem. The two thin electrodes are fine for single beam tests at 1 and 2 MV and they provide the opportunity for an empirical tolerance study. However they will have to be rebuilt for 16 beam experiments.

IMPROVEMENTS IN LIFETIME OF THE C^+ SOURCE

H. L. Rutkowski

Source lifetime is obviously a serious consideration in a driver where reliability affects the generation of power. However even in our experiments one does not want to repair the sources in a sixteen beam system more than necessary because of the down time involved. Our objectives in these experiments are:

1. Find the failure modes of the source and the associated cures.
2. Make the reliability of the source as high as possible.
3. Develop the statistical base to forecast when maintainence will be needed.

The source used until July was a three-arc source shown in Fig. 1. Since then we have used a single-arc source in the interests of having a large cathode mass that would, we hope, last longer. The three-arc source would typically last for 10K shots before needing rework because of cathode erosion into the blast shield. The new single cathode is a cylinder of POCO EDM3 graphite (1.80 g/cc) with .20" ID and .75" OD. This design is to be compared with the three-arc cathodes which were .125" diameter rods. The new design of the source was run at 350 A arc current for comparison with the three-arc source.

The diagnostic chosen for the lifetime studies was the double-slit emittance measurement system. This was regarded as the most sensitive test of source performance because the phase space of the beam is examined over many shots and the pulse shape on an individual shot depends on very local behavior in the beam so that small effects are not averaged out. A bad shot was defined as a zero signal or abnormally high signal occurring at a normally occupied point in phase space, or as an out of range signal occurring where zero signal was expected.

The source does not simply work or not work. When the performance started to degrade it would sometimes resurrect itself after a period of time. This source is not subject to what one would normally view as infant mortality. There is a conditioning period at the beginning followed by a long period of satisfactory operation. The statistical data we are looking for is the distribution of the true failures as a function of accumulated shots. About 580 shots were put on the source before the emittance scans commenced. These were done to check plasma shut off in the source and to make sure that various electronic systems were working properly. Each emittance scan consists of 900 shots about 324 of which are in the area of phase space occupied by the beam. The only way we have of detecting a malfunction in the area of no beam is to see an out of range signal or to see a misfire of the arc discharge pulse.

The history of the source experiment is complex because of the ambiguity of the failure modes and the different cures attempted. The history can be broken into 4 parts based on when major changes were made to the source. They are described as follows:

Part I 0 to 9580 shots -
A period of very reliable operation with a good shot rate of 99.6% which was interrupted in the middle for a period of one scan. The plasma switch grid was replaced at the end of this part with no other modifications to the source.

Part II 9580 to 27,600 shots -
A period of reliable operation with a 99.7% good shot rate interrupted in the middle by one scan with a 97.5% good shot rate and self recovery by the source as in Part I.

Part III 27,600 to 34,200 shots -
Degradation to 90% good shot rate at the start followed by attempts to repair the source by replacing the plasma switch grid first and then the exit grid without success.

Part IV 34,200 to 36,000 shots -
After manually cleaning the flashover trigger surface only a period of 99.7% good shot rate.

We have no explaination at present for why the plasma switch grid change at the end of Part I worked. No damage or blocked grid area was observed. The cathode was never replaced in these tests. The trigger was cleaned with a dental sand blaster.

We then performed large-aperture Faraday-cup measurements to check the total current in the beam. The total current measurements indicated that the single arc can be used at 250 A discharge current without dropping below our ion flux needs. After the current measurements four more emittance scans (3600 shots) were performed to see if the source was still functioning properly but the good shot rate dropped below 90% and attempts to improve performance by varying the plasma switch voltage failed.

In conclusion, the source runs at > 99.5% good shot rate unless there is a major problem. We have run this source four times as long as any three-arc source, identified a trigger aging effect and a possible plasma-switch aging effect. We are investigating trigger cleaning methods that can be employed without removing the source and we are performing life tests on a new source that uses tantalum trigger wires instead of the copper wires, operated at 250 A arc current.

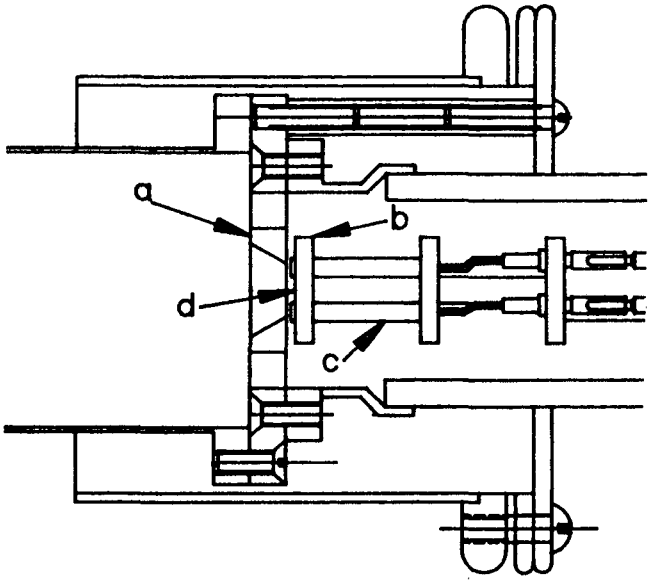

Fig. 1 Three Arc Source, a) anode, b) blast shield, c) cathode, d) trigger.

INJECTOR CONTROL SYSTEM

D.Brodzik, C. Lionberger, S. Magyary, and C. Timossi

As stated in previous papers (see ref.1), our control philosophy would mimic and benefit from the work of the ALS control group (see ref.2 and ref. 3). We will initially try to control and display Marx elements outside the pressure vessel. We have achieved control of the +/- Marx charging supplies using an ILC (Intelligent Local Controller) tied to an IBM AT (upgraded to a 386 machine) via a special 2Mbit RS485 interface (one that will be used throughout ALS). Control software consists of an Excel spreadsheet and a server program. Control values are entered into a cell in the spread sheet and sent to the ILC's DAC (digital to analogue converter) via Microsoft's Dynamic Data Exchange protocol. In a similar fashion, power supply monitored values are received from the ADC (analogue to digital converter), put into spreadsheet cells summed and displayed. A database server program is constantly exchanging data between the ILC, over the RS485 line, and Excel spread sheet. Since the operator is dealing with a spread sheet he can easily input values and change relational algorithms as needed. This means that one can take whatever data is available on the spreadsheet and combine it into an equation of current interest. This equation would be located in a convenient cell location and could be modified or deleted without extensive reprogramming. One could set and monitor the +/- generator charge voltage, calculate the source forcing voltage from this number, and then calculate the expected generator output based on a critical damping circuit equation. Given Excel's magnificent graphics, any cells on the work sheet can immediately be graphed in one of the graphical formats existing as separate windows on the spread sheet.

The next stage in the system development is to display additional monitored data. Among these data would be monitored voltage output from each of our two capacitive dividers, current in each of our two water load resistor legs and status of our water load regulating system. It is further necessary to control our pulsing system with the computer.

Our present single ILC capability is four analogue channels and 24 binary channels committed to control and monitoring external to the pressure chamber. We eventually hope to install ILC control in the high voltage dome itself. Initially all source electronics will be stand alone with local fixed reference levels.

References

1. LBL - 25985, "The Berkeley 2MV Heavy Ion Fusion Injector", pg.3.
2. The Conceptual Design Report July 1986 for the 1-2 Gev Synchrotron Radiation Source Pub-5172 Rev.
3. The Uranium Beams Project [Lancaster et al., 1979; Magyary et al., 1981a; Magyary et al., 1981b].

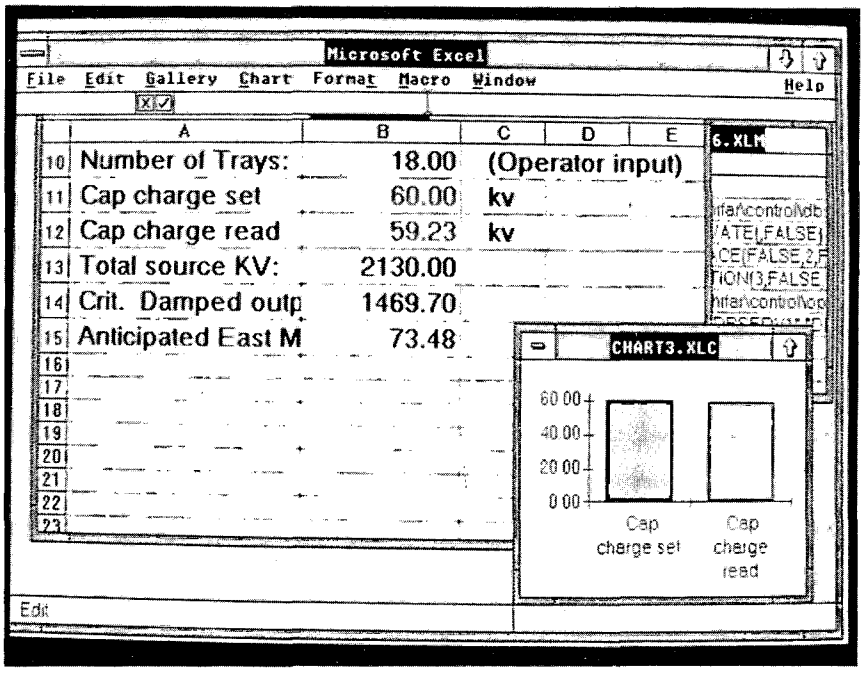

Typical Excel Spread Sheet Display.

MAXWELL SPARK GAP TEST UPDATE

J. STOKER

The past Maxwell capacitor life test[1] indicated that the life expectancy of the Maxwell spark gap was of more concern than the life of the capacitor. Although the capacitor easily survived, five gaps were used to achieve one million pulses. The best gap lasted 450K pulses, while the worst lasted only 70K pulses. The gaps that had failed were tracked inside the lexan housing from the brass electrode across the surface to the air inlet on one side and from the brass electrode to the air exhaust on the other side. The tracking had a blue and black cast as if brass was vaporizing and being deposited on the lexan. Spectroscopic analysis revealed that the contamination was mostly copper but contained 3% iron and 3% zinc.

The next test was performed using a gap with a history of less than a hundred pulses and refitted with stainless steel electrodes. The test circuit was the same with a new capacitor. This gap ran for two million pulses and was disassembled. There was no apparent tracking. The negative electrode side of the gap, which was also the air-exit side was full of brown powder. This powder appeared to be iron oxide and was magnetic. The positive electrode side was clean with no tracking. The electrodes were eroded and cupped in the center.

The defect of the next gap test was to determine if one could remachine badly tracked lexan housings. The inside of the housing was remachined with a custom made tool to retain the inside curvatures. New stainless electrodes was used. The gap lasted 400K pulses. Brown powder was present at both sides of the housing. The air flow for this gap had been reversed; the air output was on the positive electrode side.

The gap from the above test was cleaned since there was only brown powder but no tracking. The stainless steel electrodes were remachined. The air flow was arranged the same as the gap that survived 2 million pulses. This test gap lasted only 120K pulses. There was brown powder on both sides of the housing and the blue contamination reapeared. The air supply was in question although it had been tested for hydrocarbons at the beginning of these tests. There are three instrument quality air filters between the air supply and the gap. These filters were disassemble and examined and no evidence of any contamination of any kind was present.

As a final test the conditions that produced a lifetime of 2 million pulses were repeated. Others included:

1) New lexan housing with new stainless electrodes.
2) Air input side is the positive electrode side. Air exhaust is the negative electrode side.
3) The gap is positioned horizontally with the positive electrode up.
4) Electronic circuit is the same.
5) Instrument quality clean air is used to pressurize the gap.

This spark gap lasted 600 K shots. Inspection showed no brown powder and a small amount of blue contamination with many large track marks.

Conclusions and Comments

The spark gaps as supplied by Maxwell with brass electrodes can be expected to last approximately 100 K pulses. The same gaps refitted with stainless steel electrodes, in the right polarity verses air flow configuration should last 500 K pulses minimum.

The expected shot rate of the 2 MV injector does not warrent retrofitting the present spark gaps with stainless steel electrodes at the present time. The electrodes of the present spark gaps will be refitted with stainless as they are replaced.

The gap that lasted two million pulses is an unexpected curiosity that should be investigated in the future.

ILSE COSINE 2θ QUADRUPOLE MAGNET DEVELOPMENT

W. Thur

Introduction

One of the component development tasks identified in the ILSE Design Study is the fabrication of prototype current-dominated quadrupole magnets of high field quality. The requirements for these magnets are unique in several respects.

A quadrupole field is created by spacing the windings according to a Cosine-2θ function as they are wrapped around the periphery of the aperture. However, as seen by the ion beam, the outer windings have a longer effective length, and would thus exert a greater influence on the beam. This is compensated by modifying the Cosine spacings slightly. Iron laminations are used to return flux outside the aperture for increased efficiency and to attenuate end fringe fields. Field quality in the aperture is determined entirely by the physical location of the electrical currents in the individual windings.

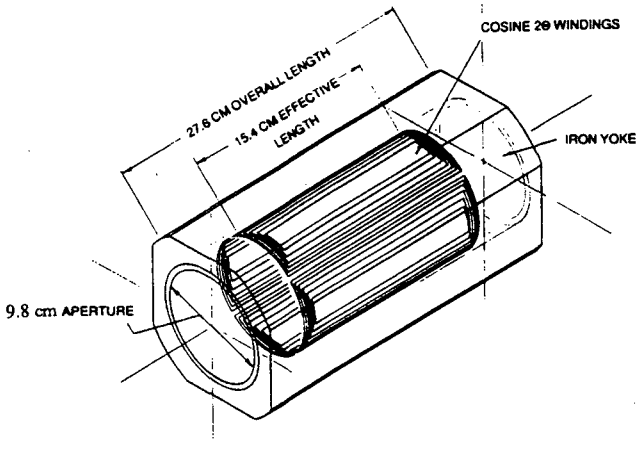

The ILSE Prototype Magnet

Design Advantages

Without conventional shaped-iron pole faces, much less radial space is needed around the effective field area. In ILSE, this allows a more closely packed matrix of multiple beams. This is a critical requirement in the magnetic focus acceleration section, where four ion beams in a square array must match the beam-to-beam spacing set by the existing injector, and must also fit through the limited diameter of the acceleration cores. The low duty-cycle pulsed operation of these magnets also helps to minimize the space needed for conductors and allows operation without a cooling system.

In a high current accelerator such as ILSE, the ion beam cross section fills a significant portion of the magnet aperture. This means that the effects of the magnet end fringe fields off the beam centerline become important to overall beam transport. The Cosine 2θ current-dominated design is much more amenable to 3-D analysis of these end fringe fields, and once analyzed, winding spacings can be altered to compensate for fringe field distortions. The goal is to achieve a magnetic field in which the path-length-integrated field is essentially the same over the entire beam cross section. In the case of a quadrupole, that is: $\int B'dl$ = constant. This is a key rationale for the use of Cosine 2θ magnets in a high-current accelerator.

The current-dominated principle allows the simple superposition of dipole and quadrupole fields. Separate Cosine θ and Cosine 2θ windings can be layered in a single magnet, giving independent control of the strength of each field. Thus, the beam-bending strength of a dipole field can be adjusted without affecting the superimposed beam-focussing quadrupole field. This is the operating principle behind the Cosine θ / Cosine 2θ combined function dipole / quadrupole magnets planned for ILSE's Bend section, which makes a 67% field "occupancy" possible. Without this high occupancy, a larger bend radius would be required.

Development Approach

An economical, reliable fabrication technique is needed to produce about 200 of these magnets for the ILSE experiments. The required parameters call for 24 turns of 2 mm copper wire (or equivalent) per pole, precisely located according to the modified Cosine 2θ distribution. This is the principal fabrication challenge: each conductor must be spatially positioned to a tolerance of about ± .003".

A variety of labor-intensive fabrication techniques exist which might be suitable for fabricating one or two of these magnets. What we are seeking, however, is a method with relatively low labor content, and built-in, reproducible accuracy in the location of the electrical windings. Some of the techniques investigated to date are chemical milling of thin-wall copper tubes, 5-axis NC machining of solid copper, laser cutting, and EDM methods. Cast plastic resin wire forms can be made to the required tolerances with good reproducibility, but the problem of forming the relatively heavy and stiff copper wire to precisely `fit into these forms has not yet been solved.

Currently, two new approaches are being explored: A laminated build-up of layers of .020" copper on kapton substrates, as used in industry for flexible printed circuit boards, and a cast plastic resin form filled with many strands of relatively fine wire connected electrically in parallel.

This development task was pursued with a low level of funding in FY89, more effort and progress is foreseen for FY90. When a satisfactory method of fabrication is developed, attention will turn to the task of measuring and mapping the magnet's field to assess its quality, and as an input for ion beam dynamics models.

ELECTROSTATIC QUADRUPOLE PROTOTYPE DEVELOPMENT ACTIVITY

S. Mukherjee

The ILSE Conceptual Engineering Design Study[1] completed in March 1989, defined an application for 16-beam electrostatic quadrupole focusing arrays. For ILSE, 32 of these quadrupoles are required for the matching, electrostatic accelerator, and beam combiner sections. In order to achieve the required beam control[2,4] the dimensional tolerance of the quadrupoles must be held to ± .002 inch as assembled. Since this assembly is made of several components whose fabrication tolerances tend to stackup, the tolerances of each part should be held close to ± .0001 inch. Achieving such tolerances presents a significant manufacturing challenge.

Two approaches were investigated during the design phase. The first was to use the newly developed technology of super plastic forming of titanium alloy sheet to produce one monolithic piece for the electrodes and the quad-plate. This required substantial research and development efforts to extend the process to form electrodes 2 inches in diameter and 8 inches long. The initial tooling cost could not be justified for a limited run of 32 quadrupole. assemblies. The second approach was to use conventional Computer Numeric Control (CNC) machining of parts and assemble them with or without the aid of simple fixturing.

Based on a CNC fabrication approach, the design of the 16-beam quadrupole was reviewed[5] on July 13, 1989. This design is shown in Fig. 1 and illustrates the following features:

1. The integrated assembly has a ground plate at each end which are biased at up to ± 50 kV dc. Each assembly contains a total of 25 electrodes distributed between the two quad-plates and separated by 6 ceramic insulators

2. Three spacer rods connect the ground plates and hold the two halves of the assemblies parallel.

3. The plates and the electrodes are of stainless steel with a surface finish better that 20 micro inches.

4. The ceramic insulators that attach each quad plate to the opposing ground plate are matched in length in sets of three.

5. The ground plates have a tangential slot cut at four places which serve as fiducials in the X-Y directions.

The most critical parameters of the CNC machining are: the close tolerances of hole-centers (± .0001 inch) for the electrodes; the roundness of these holes and the length of the three spacer rods and ceramic insulators. The parallelism between electrodes depends on the flatness of the quad plates (± .0002 inch) and the concentricity of the outer diameters of the electrode (±.0001 inch). The selection of half-inch-thick 303 stainless steel for the plates will help to achieve the surface flatness tolerance. Grinding will be used to meet the roundness tolerance of the beam holes of the diameter tolerance of the electrodes and spacer rods, and the length tolerance of the ceramic insulators. To reduce the electrical field at the triple-point junction, metal inserts will be brazed at the two ends of each insulator.

Development began in April 1989 and procurement was started in July. We expect to complete prototype assembly by the middle of October 1989. This operation will include parts cleaning and assembly in a clean room at LBL. The dimensional validation of the quadrupole assembly will be performed at a metrology specialist's facility with a capability of measuring to 1 μm ($4x10^{-5}$ inches). The software of this machine will be used to determine the best-fit center of the entire quadrupole array based on the true measured positions of all the electrodes. This will provide the basic reference of the electrostatic field center. Fiducials will be referred to that virtual center. Electrical breakdown tests in vacuum of the assembled quadrupole are scheduled to be performed in a high voltage test stand in November 1989.

References:

1. ILSE Conceptual Engineering Design Study, March 1989 - Pub. 5219.
2. L.Smith, "Electrostatic Quadrupole Misalignments in ILSE", HIFAR Note 182, Feb. 1, 1988.
3. L. Smith, "Transverse Mis-Alignment in a Driver"- HIFAR year end report, 1988.
4. L. Smith, "Tolerance on Longitudinal Position of Quadrupoles" HIFAR year end report, 1989.
5. Engineering Design Review, dated July. 13, 1989 and action items documents.

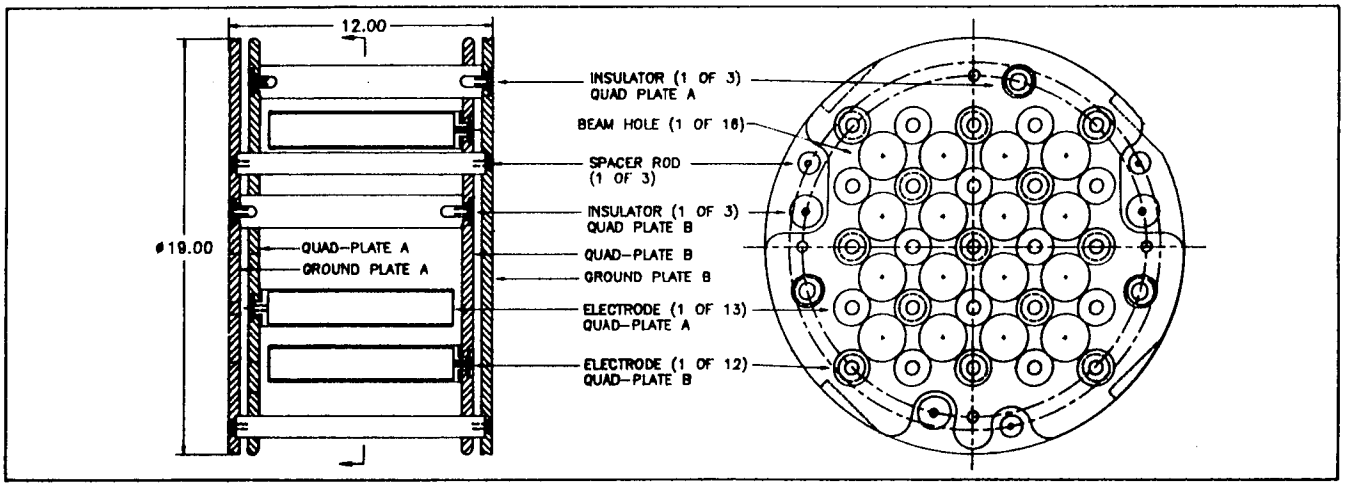

INDUCTION ACCELERATOR CELL DEVELOPMENT

C. Fong and A. Faltens

The ILSE Conceptual Engineering Design Study[1] identified the necessity for the development of an accelerator cell and its pulser. A point design effort based on ILSE design parameters commenced January 1989 and is scheduled for completion by October 1990. The development will provide an evaluation of several induction core materials under development; substantiate the engineering basis for the acceleration cells required for the ILSE sequence; and provide basic data for HIF driver economic and feasibility studies.

An important criterion for the design of driver accelerator cells is cost. Parameters which impact cost are core and pulser performance and efficiencies. The point design, fabrication, and evaluation effort has already defined cost-effective tradeoffs between core material characteristics and components for the accelerating pulsers. Based on preliminary data, a cell configuration comprised of two nested accelerator core packages driven by two 90-kV pulsers in parallel was selected. From this, basic performance parameters were then identified using Allied Signal's Metglas products as the primary induction core material.

Reductions in the price of Metglas have been accomplished through the implementation of production-based casting machines recently commissioned by Allied. Yet to be developed is a satisfacting technique of insulating the turns of the induction core. Two approaches that show promise are currently under development by Allied: 2605 CO annealed then wound with Mylar and 2605 S2 coated with a solvent based polyimide then annealed. The CO series appears to meet the efficiency and cost envelopes for ILSE but because of its cobalt content may prove to be to costly for a full scale driver. The S2 approach holds the promise of not only being efficient but also relatively inexpensive due to its iron-based formulation. However, its success depends on the development of an inexpensive interlaminar insulation capable of surviving annealing.

We have begun a series of electrical tests to characterize 2605 S2 wound with Kapton on small bench sized cores. These tests will be used to aid in the selection of the core material and provide data for the design of the 90 kV pulsers.

Figure 1 shows a quadrant cross section of the cell point design. Wound Metglas is arranged in a nested inner/outer configuration to minimize axial packaging as required in ILSE's electric focus sections. The two cores are driven by two 90 kV pulsers in parallel. Metglas, in its post annealed state, has limitations in mechanical stresses due to its anisotropic magnetostriction properties. Moreover, with winding tension minimized, the Metglas has a propensity to slide against itself or "cone". A semi rigid core container has been designed to support the Metglas from both its inside and outside diameters, with sideplates to contain limited coning. Both cores will be wound on mandrels which will then be annealed and/or assembled into core packages by Allied for shipment. The core packages are then sequentially assembled, pumped to vacuum and backfilled with a freon dielectric fluid. Since freon degradation due to corona is anticipated, a freon circulation system is required. Incipient fluid failures through mechanical joints such as a freon or vacuum leak would be to/from atmosphere. Failure of the gap insulator would cause leakage of freon to the beamline - a much easier cleanup as compared to transformer oil. Other insulators are arranged to also accept vacuum and hydrostatic loads. Handling and seismic loads have also been considered.

A parallel pulser configuration was selected after considering 1-μsec pulse widths, the availability of 90- to 200-kV commercial spark gaps and capacitors, lifetime and derating factors, and the various core arrangements based on standard Metglas ribbon widths. This point design, based on the existing MBE-4 pulser rated at 60 kV parallel, is to provide 90 kV for pulses within a 5% variance. Current efforts consist of finding sources for the critical components.

Future work will consist of: continued activities to characterize Metglas materials; fabrication of cell piece parts; development of gap diagnostics; and continued development of coating, winding, annealing and assembly techniques with Allied.

Reference

1. ILSE Conceptual Engineering Design Study, March 1989 - Pub. 5219.

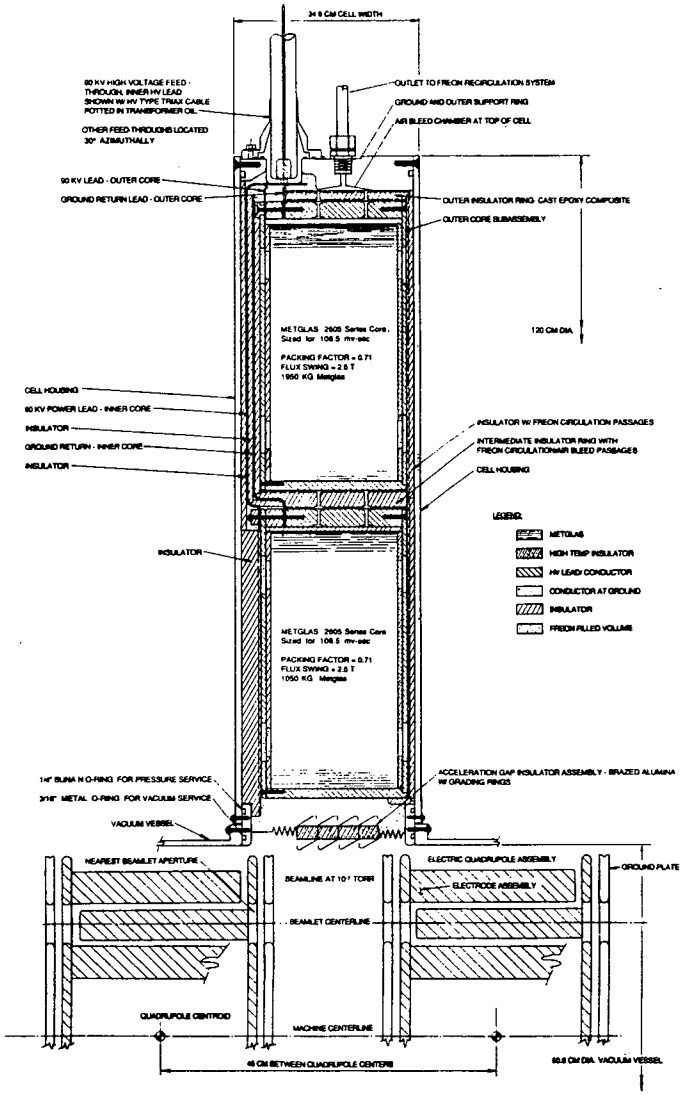

Fig. 1 ILSE Electrostatic Accelerator Cell.

EFFECT OF A SPREAD IN BEAMLET CURRENTS ON LONGITUDINAL STABILITY

K. Hahn and L. Smith

Introduction

It is predicted[1] that, under some conditions, perturbations of beam current in a heavy ion driver can be amplified by their interaction with the resistive component of impedance from the accelerating modules. There are several strategies for controlling or even eliminating this undesirable mode growth, including introduced momentum spread, designed low impedance, and feedback on accelerating waveforms. An additional mechanism for reducing growth rates, recently pointed out by Bruce Langdon (LLNL), is to vary the phase velocities of space charge waves among the (N) multiple beamlets in the overall current pulse. This is most easily accomplished by varying the beamlet currents at injection and may be reasonably simple in practice.

From a mathematical viewpoint the effect of varied phase velocity amounts to a spreading of a resonance factor among the N beamlets so that only one at a time can be strongly excited. That is, a factor in the mode dispersion relation (see Eq. (3) below), normally of the form $N\, v_p^2 / \left(\omega^2 - k^2 v_p^2\right)$ is replaced by the sum over beamlets (i - 1, ... N)

$$\sum_{i=1}^{N} v_{pi}^2 / \left(\omega^2 - k^2 v_{pi}^2\right) \qquad (1)$$

Here $\omega(k)$ is the mode frequency for wave number k defined in the beam frame and $v_{pi}^2 = \frac{q^2 \lambda_{oi}\, g_i}{m}$ is the space-charge-wave phase velocity for the ith beamlet. If the currents are varied sufficiently then mode growth rate can drop by up to a factor of N^{-1}. This property is quantified in the following simple formulation of the instability.

Equations

The linearized fluid equations in the beam frame lead to an equation for the perturbed line number density of the i^{th} beamlet (assuming $e^{i(kz-\omega t)}$ dependence):

$$\lambda_i = - ir \frac{v_{pi}^2}{\left(\frac{\omega}{k}\right)^2 - v_{pi}^2} \sum_{j=1}^{N} \lambda_j \,, \quad \text{where } r = \frac{4\pi R \beta_o}{Z_o g k} \,. \qquad (2)$$

Here R is the module resistance in ohms/m. Since the beamlets now have separate identities, Eq. (2) is a set of N equations for N modes. The characteristic equation for the N frequencies is obtained by summing both sides of Eq. (2):

$$1 = - ir \sum_{1}^{N} \frac{v_{pi}^2}{\left(\frac{\omega}{k}\right)^2 - v_{pi}^2} = - ir \sum_{1}^{N} \frac{\beta_i}{\alpha - \beta_i} \qquad (3)$$

where $\alpha = \left(\frac{\omega}{k\bar{v}_p}\right)^2$, $\beta_i = \frac{v_{pi}^2}{\bar{v}_p^2} = \frac{I_i}{\bar{I}}$ and $\sum_{1}^{N} \beta_i = N$.

Limiting cases can be seen from Eq. (2). If r = 0, the beamlets are uncoupled, each with frequency $\omega = \pm k v_{pi}$. If the currents are all the same, there is one mode with equal λ's and $\left(\frac{\omega}{k}\right)^2 = v_p^2[1\text{-}iNr]$ and N-1 modes with $\sum_{1}^{N} \lambda_i = 0$ and $\omega = \pm k v_p$.

We can also anticipate that if r is small compared to the fractional spread in current, the beamlets are again decoupled with $\left(\frac{\omega}{k}\right)^2 \approx v_{pi}^2\,[1\text{-}ir]$. This is a consequence of the fact that a purely resistive impedance reacts instantaneously; the various perturbations arrive at a module at different times and the module reacts to each one separately. If the wake field were included in the analysis the coupling could be significant. Finally, it can be seen from the form of Eq. (3) that the N solutions for α satisfy the relation:

$$\sum_{1}^{N} \alpha_i = N[1\text{-}ir] \qquad (4)$$

This says that some modes must be unstable; at best, there can be several modes with low growth rates instead of one with a large growth rate.

Numerical Results

Finding 16 roots of Eq. (3), corresponding to current driver scenarios, is a tedious job, to put it mildly. We have looked at N≤4 to get a qualitative idea of the effect of a spread in beamlet currents. Table 1 gives a summary of the solutions of the sample cases where the maximum fractional current spread is ±7.5%. The circuit coupling strength r is varied from 0.002 to 2. Both limiting cases of large and small r show the expected characteristics of the previous section. The summation of α satisfies Eq. (4) for all the cases. When r=0.02 the largest imaginary $\alpha \sim Nr/2$. This suggests that the r should be of the order of the fractional current spread in order to have some de-coupling of the beamlets to the external circuit.

Discussion

For typical parameters of a heavy ion fusion driver, R ~ 100 $\frac{\Omega}{m}$, $\beta \sim 0.3$, g ~ 2, $k = \frac{2\pi}{\lambda} \sim 0.3\ m^{-1}$, and the coupling strength r ~ 2. Thus the beamlets are strongly coupled and the largest growth factor is $\mathrm{Im}[\alpha] \approx Nr$. If the resistance can be sharply reduced by some means, a spread in currents might help to reduce the growth rates further.

Table 1 Roots of Eq. (4) for N = 2 and 4.

r	N	α (real,imaginary)			
2.0	4	(0.943,	-0.00012),	(0.999,	-0.00014),
		(1.00,	-8.00),	(1.055,	-0.00012)
0.02	4	(0.936,	-0.011),	(0.991,	-0.0226),
		(1.011,	-0.034),	(1.061,	-0.0124)
0.002	4	(0.925,	-0.00184),	(0.975,	-0.0020),
		(1.025,	-0.0021),	(1.075,	-0.0021)

Reference:

1. L. Smith, " Resistive Instability Growth Rates," HIFAR Note 217, Sept. 88.

HEAVY ION LINAC DRIVER ANALYSIS

E. Lee, E. Close, and W. Thur

A preliminary version of HILDA has been written and is currently being tested using an improved beam dynamics model along with a simple accelerator and component cost model. Realistic models are being developed. A standard subroutine template has been established to assist in the writing and documentation of the processes, see Figure 1. This template has been used to build the main subroutine Dcost1 which is a closed-loop event-driven driver shown schematically in Figure 2.

Also, subroutines to calculate the minimum cost at a user specified driver module station have been written. These are based on a simple preliminary beam-dynamic/ structure-cost model which is thought to contain the program features. The basic program module is CalCost shown in Figure 3. This module uses a number of sub-modules which are listed in Figure 4, along with some miscellaneous subroutines shown in Figure 5.

Also, a format for parameter data files has been established. This will allow easy user editing of program data files and at the same time permit these files to be read and edited by the HILDA data processes from within HILDA.

The documentation of HILDA is being done concurrently with the program development by following a consistent format of process writing along with maintaining a Microsoft Word document that contains all notes, conventions, and the actual subroutine source listings. These listing can be down-loaded to create the source code which will compiled with no further editing.

Figure 1: Shortened version of the template:

```
c  FILE: template.ALL
c  This is the complete file for a processes:
c  Each template section is logically a file with
c  identification  fileName.fileType

c SUMMARY
c  Contains a concise description of the  process.

c PROCESS I/O
   SUBROUTINE template
    (task, pIN1, pIN2, pINn,
    pOUT1, pOUT2, pOUTm)
c  Define the process header and the IO variables:

c DESCRIPTION
c  Documentation of the process: .

c CONSTANTS
c  Constants  used:

c EXTERNAL PROCESSES
c  Declare  global processes:

c LOCAL VARIABLES
c  Declare  Local variables:

c PARAMETER DATA
c  Parameters that can be assigned values from a file:

c LOGIC AND EQUATIONS WITH COMMENTS
c  The executable section
   RETURN
   END
```

Figure 2: Main Subroutine Dcost1.

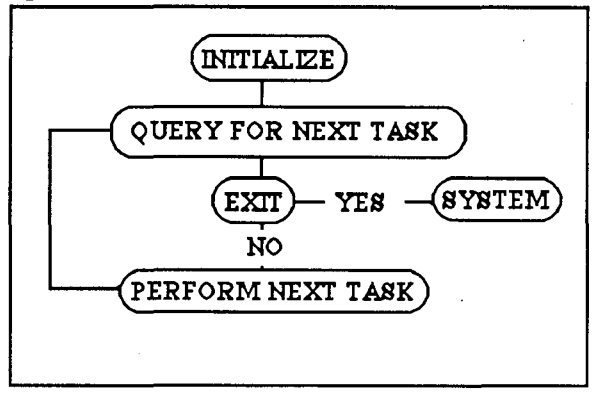

Figure 3: Module CalCost

CalCost
Open Files
Fetch Beam Parameter Data
Compute the Minimum Cost Configuration
Update/Save Calculation Results

Figure 4: Sub-modules

CostV1	Cost at a given energy, i.e. station
KinVar	Kinetic variables
CostLadV	Cost at given period, beam size, voltage
REPhi	Dynamic variables R, eta, and Phi
alSiggaBar	Dynamic variables alpha, sigma, alpha
QIT	Perveance, current, pulse length
StrucCore	Structure and Core quantities
CostCalc	$ cost per volt

Figure 5: Miscellaneous utilities:

FileName	Create file names as needed
MenuList	Display a menu of available tasks
DataLU	Data reading routine
DataFN	Data reading routine
DataUpDate	Data updating routine

PUBLICATIONS AND INTERNAL NOTES

HIFAN-388
LBL-25047
Lee

E. P. Lee and J. Hovingh
"Heavy Ion Induction Linac Drivers for Inertial Confinement Fusion," Fusion Technology 15, No. 2, part 2A, 369 (1989).

HIFAN Note-430
Fessenden

T. Fessenden
"Available Background Material for the NAS Review of Inertial Fusion: Heavy Ion Fusion," May 1989.

HI-FAN-431
LBL-27230
HIF Staff

HIF Staff
Heavy Ion Fusion Accelerator Research (HIFAR) Half Year Report October 1, 1988 - March 31, 1989 (June 1989).

HIFAN Note-432
Keefe

D. Keefe
"A program Briefing for The National Academy of Science Review of Inertial Fusion," July 18-19, 1989

HIFAN Note-433
LBL-27455
Eylon

S. Eylon, T. Fessenden, T. Garvey, and H. Meuth,
"Beam Dynamic Studies in the Multiple Beam Experiment MBE-4" July, 1989, abstract submitted to the Thirty-First Annual Meeting Division of Plasma Physics, Nov. 13-17, 1989. (LBL report submitted by MFE Group).

HIFAN-434
HIFAR Group

"NAS ICF Review Briefing Book, August 16, 1989"

HIFAN-435
Keefe

D. Keefe
"Foreign Travel Report: NAS Panel for Review of Inertial Confinement Fusion, Washington, D.C., July 18-19, 1989"

HIFAR NOTES (Internal and Informal)

HIFAR Note-237
Johnson
R. Johnson, S. Eylon, and H. Meuth,
"Survey & Alignment of MBE-4," Dec. '88 - Jan. '89.

HIFAR Note-238
Brady
V. Brady,
"Perturbed Electrostatic Quadrupole II," (4/12/89).

HIFAR Note-239
Stoker
J. Stoker,
"Injector Marx Spark Gap Life Test," (5/12/89).

HIFAR Note-240
Faltens
A. Faltens and K. Hahn,
"Effects Which May Contribute to Emittance Growth and Beam Displacement," (5/18/89).

HIFAR Note-241
Stoker
J. Stoker,
"Maxwell Spark Gap Tests Update," (7/20/89).

HIFAR Note-242
Brodzik
D. Brodzik,
"Status and Directions," (7/25/89).

HIFAR Note-243
Meuth
H. Meuth and C. Lionberger,
"High-Resolution Diagnostics on MBE-4 with the TEKTRONIX 602 Oscilloscope," (8/7/89).

HIFAR Note-244
Lionberger
C. Lionberger
"MBE-4 Program Conversion from Tek 7020 to Tek 11602," (8/7/89).

HIFAR Note-245
Fessenden
T. Fessenden,
"Transverse Emittance Growth in MBE-4," (9/1/89).

HIFAR-Note-246
Chupp
W. Chupp,
"MBE-4 Source Modifications and Maintenance procedures," (9/89).

HIFAR-Note-247
Hahn

K. Hahn,
"Effect of a Spread in Beamlet Currents on Longitudinal Stablity," (9/89).

H.I.F. STAFF ROSTER

Denis Keefe

Donald A. Brodzik
Warren Chupp
Robert D. Edwards
Andris Faltens
Thomas J. Fessenden
Craig Fong
Robert Fulton
Terence Garvey
Ron Gervasoni
William B. Ghiorso
Wayne Greenway
Michael Gross
Ralph Hipple
Cai Houston
Rudin Johnson
Brian Lipps
Carl Lionberger
Hermann Meuth
Sam Mukherjee
Harry Meyer
Joseph Perez
Chester D. Pike
John Pruyn
Thomas Purtell
James Rice, Jr.
Henry L. Rutkowski
Gerald L. Stoker
William Thur
Bill Tiffany
David Vanecek
Richard Weidenbach
Gerald West
Mark Zbinden

Lloyd Smith

Victor Brady
Elon Close
Kyoung Hahn
Enrique Henestroza
David L. Judd
L. Jackson Laslett
Edward P. Lee

Clerical Staff

Martha Condon
Joy Kono
Alline Tidwell
Olivia Wong

Visiting Participants

LANL

E. Meyer

RAFAEL

Shmuel Eylon

SLAC

William B. Herrmannsfeldt

UNM

S. Humphries

HALF-YEAR/YEAR-END REPORT: DISTRIBUTION LIST

Allied Chemical Corporation

C. Smith

Argonne National Lab.

T. A. Fields
R. Martin

University of Arizona

R. Morse

Batelle

J. Hartman

BMD/ATC/SDC

M. Hawie
B. Strickland

Brookhaven National Laboratory

M. Barton
E. Courant

C.E.A. Bruyeres-le-Chatel

R. Dei-Cas

CEBAF

J. Bisognano
D. Douglas
H. Grunder
G. Krafft
C. Leemann

CERN

C. Rubbia, Director-General
E. Picasso, EP
D. Mohl

University of Calif., Irvine

N.Rostoker

Cornell University

D. Hammer
J. Nation
R. N. Sudan

DARPA

H. Lee Buchanan

Department of Defense (SDIO)

R. Gullickson
M.Toole

Department of Energy

DP-OIF

G. D'Alessio (DP-DIF)
S. L. Kahalas (DP-DIF)
R. Shriever (DP)
M. Sluyter (DP)

Department of Energy (Con't.)

ER

R. Gajewski (AEP)
G. Peters (HENP)
W. Polansky (AEP)
R. Rader (OPA)
D. Stevens (BES)
D. F. Sutter (HENP)
J. Decker, (ER-2)
A. Davies (OFE)

DOE San Office

R. Bredderman
D. Neely

E.P.R.I.

R. Scott

Fermi National Accelerator Lab.

F. T. Cole
F. Mills
L. Teng

F.O.M. Amsterdam

F. Siebenlist

Fusion Power Associates

S. Dean

GANIL

P. Lapostolle

GE

J. Lucek

GHG Associates

G.H. Gillespie

GSI

R. Bock
D. Boehne
I. Hofmann

University of Illinois

G. Miley

Institut fuer Kernphysik

H. Meuth

Institute for Nuclear Study

Y. Hirao
T. Katayama

Kanazawa University

S. Kawasaki

Lawrence Berkeley Laboratory

J. Alonso
D. Attwood, 80/101
K. Berkner, 50/149
D. Brodzik, 46/125
C. Celata, 47/112
W. Chupp, 47/112
J. Chew, 50/149
S. Chattopadhyay, 47/112
T. Elioff, 90/4040
A. Faltens, 47/112
T. Fessenden, 47/112
C. Fong, 47-112
R. Fulton, 90-2148
A. Garren, 90/4040
T. Garvey, 47/112
R. Gough, 50/149
K. Hahn, 47-112
R. Johnson, 50A/4119
D. Judd, 47/112
D. Keefe, 47/112
C. Kim, 47/112
M. Krebs, 50A/4112
W. Kunkel, 4/230

Lawrence Berkeley Laboratory (Con't)

G. Lambertson, 47/112
L.J. Laslett, 47/112
E.P. Lee, 47/112
C. Lionberger
E. Lofgren, 47/112
J. Marx, 46/161
J. Meneghetti, 46/161
S. Mukherjee, 47-112
P. Oddone, 47/112
C. Pike, 47/112
H. Rutkowski, 47/112
A. Sessler, 4/230
C. Shank, Director, 50A/4133
L. Smith, 47/112
C. Taylor, 46/161
W. Thur, 47-112
D. Vanecek, 58/101
A. Warwick, 46/161

Lawrence Livermore Laboratory

R. Bangerter, L-477
W. Barletta, L-626
W. Fawley, L-626
A. Friedman, L-630
A. Glass, L-1
D. Hewitt, L-472
D. Ho, L-477
W. Kruer, L-472
W. Krupke, L-488
B. Langdon, L-472
J. Lindl, L-477
J. Mark, L-477
J. Nuckolls, Director, L-295
L. Reginato, L-627
E. Storm, L-481
D. Prosnitz, L-626
S. Yu, L-626

Legnardo Laboratory

R.A. Ricci

Lockheed

J. Siambis

Los Alamos National Laboratory

I. Bohachevsky
R. Cooper
R. Jameson
T. McDonald
E. Meyer
R. B. Perkins
R. Stokes
T.-S. Wang
D. Wilson

University of Maryland

M. Reiser
D. Tidman

Max Planck Inst. fur Plasma Physik Garching

A. Schluter

Max-Planck-Inst. fur Quantenoptik

J. Meyer-Ter-Vehn

Maxwell Laboratories

Library

University of Nagaoka

K. Yatsui

University of Naples

G. Vaccaro

National Institute of Standards Technology

S. Penner
M. Wilson

Naval Research Laboratory

S. Bodner
T. Coffey, Director
T. Godlove
I. Haber
P. Sprangle

Osaka University, Institute of Laser Engineering

T. Mochizuki
S. Nakai, Director
C. Yamanaka

University of Padova

G. Ricci
A. Pascolini
M. Pusterla

University of Paris at Orsay

C. Deutsch

Physics International

Library

Pulse Sciences, Inc.

I. Smith
K. Nielson
M. Tiefenback

RAFAEL

J Shiloh

Rutherford Laboratory

J. D. Lawson
C. Pryor
G. Rees

Sandia Laboratories

E. H. Beckner
D. Cook
G. Kuswa
T. Martin
J.P. VanDevender
K. Prestwich
M. Clauser
G. Yonas

SLAC

D. Gough
W. Herrmannsfeldt, Bin 26
B. Richter, Director, Bin 7

Soka University

T. Saito

SOREQ Nuclear Research Center

A. Sternlieb

SSC

R.J. Briggs

SURA

W. Wallenmeyer, President

TITAN Systems, Inc.

K. Billman

University of TRIESTE

M. Puglisi

TRW

J. Gordon
Z. Guiragossian
J. Maniscalco
A.W. Maschke
W. Steele

UCSD

K. Brueckner
M. Rosenbluth

University of Texas at Austin

T. Tajima

URA

E. Knapp

Varian

S.S. Rosenblum

Westinghouse

M. Nahemow
E. W. Sucov

University of Wisconsin

G. Kulcinski
G. Moses
R. Peterson

Other

J.E. Leiss

LAWRENCE BERKELEY LABORATORY
TECHNICAL INFORMATION DEPARTMENT
1 CYCLOTRON ROAD
BERKELEY, CALIFORNIA 94720